Macromolecules

ARTICLE

pubs.acs.org/Macromolecules

Block Copolymer Surfactants in Emulsion Polymerization: Influence of the Miscibility of the Hydrophobic Block on Kinetics, Particle Morphology, and Film Formation

Alexandra Muñoz-Bonilla,[†,‡] Syed Imran Ali,[†] Adolfo del Campo,[§] Marta Fernández-García,[‡] Alex M. van Herk,[†] and Johan P. A. Heuts*[,†]

[†]Laboratory of Polymer Chemistry, Eindhoven University of Technology, P.O. Box 513, 5600 MB Eindhoven, The Netherlands

[‡]Instituto de Ciencia y Tecnología de Polímeros (CSIC), C/Juan de la Cierva 3, 28006 Madrid, Spain

[§]Instituto de Cerámica y Vidrio (CSIC), C/Kelsen 5, 28049 Madrid, Spain

ABSTRACT: A brush type amphiphilic block copolymer of polystyrene-*b*-poly[poly(ethylene glycol) methyl ether methacrylate], PS_{40}-*b*-$PPEGMA_{70}$, obtained via ATRP was used as stabilizer in the emulsion polymerization of methyl methacrylate. It was shown that the incompatibility between the growing polymer particles of poly(methyl methacrylate) and the hydrophobic segment of the block copolymer surfactant (polystyrene) affects both the kinetics of the emulsion polymerization and the resulting particle morphologies. Because of the incompatibility of the two polymers, phase separation occurs, and the particle morphology changes from roughly spherical core−shell to more irregular with particles containing clusters of block copolymer surfactant as the amount of block copolymer surfactant increases. This in turn has an effect on the film formation, which results in turbid films. The results obtained from the emulsion polymerization of methyl methacrylate, the obtained hairy latex particles, and the film formation process were compared with those obtained in the emulsion polymerization of styrene where both the core of the particles and the hydrophobic segment of the block copolymer are the same polymer. In this case spherical and monodisperse particles are obtained irrespective of the block copolymer surfactant concentration, and transparent films are formed after annealing above the glass transition temperature.

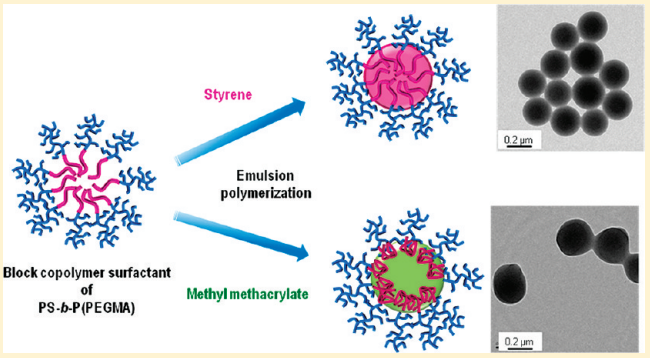

INTRODUCTION

The use of polymeric surfactants, mainly amphiphilic block copolymers, as stabilizers in emulsion polymerization[1−4] has attracted attention because of several advantages imparted to the properties of the resulting latex. Amphiphilic block copolymers exhibit unique properties in aqueous solution owing to their low critical micelle concentration (cmc) and low diffusion coefficient compared to those of conventional low molecular weight surfactants. Furthermore, the use of high molecular weight block copolymers as surfactants in emulsion polymerization can lead to the preparation of hairy particles with a core−shell structure.[5] Whereas the hydrophilic segments of the block copolymer provide the colloidal stabilization of the polymer particles along with a specific surface functionality, the hydrophobic segments strongly adsorb or anchor to the polymer−water interface, and therefore relatively long hydrophobic lengths are expected to be more efficient. In this sense the compatibility or miscibility between the hydrophobic block and the growing polymer particle is a very relevant parameter that determines how the amphiphilic block copolymer is anchored to the particle surface.[1]

We previously reported the synthesis of hairy particles by the emulsion polymerization of styrene (S) using amphiphilic block copolymers of polystyrene-*b*-poly[poly(ethylene glycol) methyl ether methacrylate] (PS_{40}-*b*-$PPEGMA_{70}$) as stabilizers.[5] In this previously reported study, the hydrophobic polystyrene (PS) blocks are miscible with the PS latex particles, and under the appropriate experimental conditions this block copolymer acts as efficient surfactant obtaining monodisperse and spherical hairy latex particles. In the present study, the synthesized PS_{40}-*b*-$PPEGMA_{70}$ brush-type block copolymer was used as a stabilizer in the emulsion polymerization of methyl methacrylate (MMA). In this case the hydrophobic PS segment is different from the polymer in the growing latex particles, PMMA, and since PS and PMMA are immiscible, an incompatibility effect may occur and the mechanism of the emulsion polymerization could be affected. The purpose of the work is to evaluate in detail the surfactant properties of the synthesized brush type block copolymer in the emulsion polymerization of MMA and to study the effects of this incompatibility during the emulsion polymerization and once the hairy particles or core−shell structure are formed. In addition,

Received: March 18, 2011
Revised: April 19, 2011
Published: May 05, 2011

the film formation process involving the resulting hairy latex particles is investigated. Related to this work are several reported investigations on composite particles (containing two or more individual polymers) consisting of incompatible phases prepared by seeded emulsion polymerization[6−10] where the morphology of these particles depends on the polymerization conditions.[11−14] Also, the film formation process of the composite latices is more complicated than that of a homogeneous latex,[15−23] and the phase separation process between the distinct polymers may affect the quality of the films.[24−29] However, to the best of our knowledge, no work has been published on the morphology of the latex containing block copolymer stabilizers with an incompatible hydrophobic segment. This system is more complex than "conventional" composite particles, now containing three polymers, two of which now connected in a block copolymer.

EXPERIMENTAL SECTION

Materials. The amphiphilic block copolymer polystyrene-*b*-poly[poly(ethylene glycol) methyl ether methacrylate] (PS_{40}-*b*-$PPEGMA_{70}$) was synthesized using sequential atom transfer radical polymerization of styrene and poly(ethylene glycol) methyl ether methacrylate (M_n = 1100 g mol^{-1}) as previously reported.[5] Methyl methacrylate, MMA (99%, Aldrich), and styrene, S (99%, Aldrich), were purified by passing over a basic alumina column. Ammonium persulfate (98%+, Aldrich) and sodium thiosulfate (99%+, Sigma) were used as received. The dialysis tubing (with cutoff molecular weight of 3500 g/mol) was purchased from Serva. Tetrahydrofuran was of AR grade and supplied by Biosolve.

Preparation of the Micellar Solution. In a typical procedure, the micellar solution was prepared by dissolving the block copolymer in a few drops of THF, and subsequently distilled water was added dropwise with vigorous stirring. The sample was transferred to dialysis tubing, sealed, and dialyzed against distilled water to remove the THF. The water surrounding the tubing was changed several times.

Emulsion Polymerization of Methyl Methacrylate with PS_{40}-*b*-$PPEGMA_{70}$ Block Copolymers as Stabilizers. All the emulsion polymerizations of methyl methacrylate (overall solids contents of 16.6%) were carried out in batch, in a three-neck reactor with an argon inlet and a mechanical stirrer. All emulsion polymerizations were carried out at block copolymer concentrations higher than the cmc (= 0.2 mg mL^{-1}).[5] A typical recipe for the emulsion polymerization of MMA using the block copolymer surfactant is as follows: the micellar solution (containing between 60 mg (7.4×10^{-4} mmol) and 460 mg (5.7×10^{-3} mmol) of block copolymer in water) was added to the double-walled reactor, and the remainder of the water needed to reach a total of 22 g of water was added. The monomer, MMA (5.000 g), was added dropwise into the reactor, and the mixture was purged with argon for 30 min while stirring. The deoxygenated solution was heated at 35 °C. The redox initiator solution (0.042 g of ammonium persulfate and 0.042 g of sodium thiosulfate in 3 g of water) was injected to start the polymerization. The argon flow was maintained throughout the reaction. At different reaction times, aliquots were extracted by syringe. A small amount of hydroquinone was added to these aliquots to quench the radical polymerization, and the monomer conversion was determined by gravimetry.

Measurements. Size exclusion chromatography (SEC) analyses were carried out on a Waters Alliance system equipped with a Waters 2695 separation module, a Waters 2414 refractive index detector (40 °C), and a Waters 486 UV detector at 60 °C. Dimethylformamide containing 0.05 M LiBr was used as eluent at a flow rate of 1 mL min^{-1}. The molecular weights were estimated against polystyrene standards. The particle size distributions were determined by dynamic light scattering (DLS) using a Malvern Zetasizer Nano ZS instrument at 25 °C. Malvern Dispersion Software was used for data acquisition and analysis, applying the general purpose algorithm for calculating the particle size distribution. Transmission electron microscopy (TEM) measurements were performed on a FEI Tecnai 20, type Sphera TEM instrument (with a LaB_6 filament, operating voltage = 200 kV). A 3 μL latex sample was deposited on a copper grid. A negative staining procedure using uranyl acetate was used to enhance the contrast. The particle size distributions were obtained from statistical treatment of representative TEM images for each sample using the software ImageJ. Average particle diameters and polydispersities were determined from these particle size distributions. Latex particle films were prepared by dip coating onto a silicon wafer substrate, and the roughness of the films was investigated by atomic force microscopy (AFM). The AFM images were obtained with a Multimode Nanoscope IVa, Digital Instrument/Veeco operated in tapping mode under ambient conditions. Glass transition temperatures (T_g) of the dried latex particles containing the block copolymer surfactant were determined using differential scanning calorimetry (DSC) on a TA Instruments Q100. Samples of 3 mg were scanned at 10.0 °C/min under dry nitrogen (20 cm^3/min). The samples were cooled from room temperature to 10 °C and maintained at this temperature for 1 min. From this temperature, they were heated to 150 °C and then cooled down to 10 °C at the same rate and repeated again.

RESULTS AND DISCUSSION

We previously reported the emulsion polymerization of S using brush-type amphiphilic copolymers, PS_{40}-*b*-$PPEGMA_{70}$, as surfactant, where the hydrophobic segment of the copolymer is compatible with the polystyrene latex particles.[5] In this article the emulsion polymerization of MMA stabilized by PS_{40}-*b*-$PPEGMA_{70}$ was carried out in order to evaluate the ability of the copolymer to stabilize PMMA, which is incompatible with the PS hydrophobic block of the copolymer. The reactions were performed using a redox initiator system, 0.8 wt % of ammonium persulfate/sodium thiosulfate at 35 °C. The amount of block copolymer stabilizer ranged from 1.2 to 9.2 wt % with respect to MMA monomer. As expected, the rate of polymerization increases with increasing stabilizer concentration (Figure 1). At low concentration of polymeric surfactant, 1.2 wt %, the formation of large amounts of coagulum was observed at relatively low monomer conversion, ∼30%, suggesting that the concentration of surfactant is not enough to stabilize the polymer particles. Increasing the polymeric surfactant concentration solves this problem, but at a concentration of 9.2 wt % relative to MMA monomer coagulum (∼10% of the total polymer amount) occurs at very high monomer conversion.

As expected, the diameter measured by DLS decreases as the amount of surfactant is increased (see Figure 2 and Table 1), but the particle size of the latex containing the largest amount of stabilizer seems to be unreasonably small. Furthermore, the particle size distributions slightly broaden as the particle size decreases, but the normalized coefficient of variation (POLY) remains close to 0.1, so we may conclude that the particle size distributions remain monomodal.

In addition to dynamic light scattering, the particle size was also determined by TEM. As can be seen from Table 1, the diameters obtained by TEM are smaller than those obtained by DLS because the latter technique measures the hydrodynamic diameter including the solvated layer of the hydrophilic PPEGMA layer, whereas this layer will be collapsed onto the particle in a TEM measurement. The TEM images of all the PMMA latex particles are shown in Figure 3.

Table 1. Summary of Particle Size and Molecular Weight Data of the PMMA Latexes Stabilized with PS_{40}-*b*-$PPEGMA_{70}$ Surfactant

surfactant (wt %)	D_{DLS}[a] (nm)	$POLY_{DLS}$[b]	D_{TEM}[c] (nm)	PDI_{TEM}[d]	$M_w \times 10^{-5}$[e] (g mol^{-1})	$N_p \times 10^{-16}$[f] (L^{-1})	$R_{pp} \times 10^{17}$[g] (min^{-1})
3.2	462	0.01	345	1.01	14.9	0.7	14.3
5.2	344	0.03	307	1.03	13.6	0.9	17.3
5.5	286	0.11	229	1.21	12.7	2.2	7.5
7.2	260	0.12	205	1.28	10.8	3.1	6.5
9.2	133	0.14	91	1.03	11.6	35.8	0.7

[a] *Z*-average particle diameter obtained from DLS using Malvern Dispersion Technology Software for data acquisition and analysis, applying the general purpose algorithm for calculating size distributions. [b] Associated normalized coefficient of variation. [c] Number-average particle diameter determined from TEM using the software ImageJ. [d] Polydispersity index of the particle size distribution determined via TEM: $PDI_{TEM} = D_w/D_n$, where D_w is the weight-average diameter, $D_w = \Sigma n_i D_i^4/\Sigma n_i D_i^3$, and D_n is the number-average diameter, $D_n = \Sigma n_i D_i/n_i$ (n_i is the number of particles with diameter D_i). [e] Weight-average molecular weight of the product polymer determined by SEC relative to PS standards. [f] N_p = number of particles per liter latex. [g] R_{pp} is the rate of polymerization per particle, here defined as $R_{pp} = R_p/N_p$.

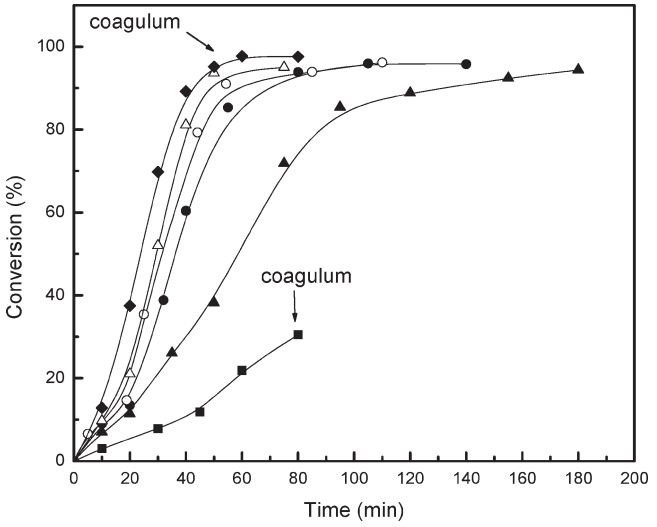

Figure 1. Evolution of monomer conversion with time for the emulsion polymerization of methyl methacrylate using a redox initiator system ammonium persulfate/sodium thiosulfate (0.8 wt %) and (■) 1.2, (▲) 3.2, (●) 5.2, (○) 5.5 (Δ), 7.2, and (◆) 9.2 wt % of PS_{40}-*b*-$PPEGMA_{70}$ block copolymer as stabilizers.

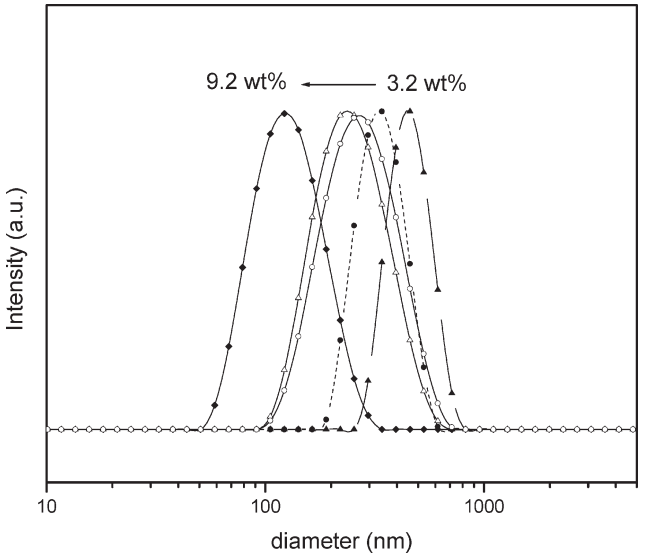

Figure 2. Intensity particle size distribution for the latex particles stabilized by (▲) 3.2, (●) 5.2, (○) 5.5, (Δ) 7.2, and (◆) 9.2 wt % of PS_{40}-*b*-$PPEGMA_{70}$ block copolymer determined using Malvern Dispersion Technology Software for data acquisition and analysis, applying the general purpose algorithm for calculating the size distributions.

Spherical and monodisperse particles were obtained using 3.2 wt % of PS_{40}-*b*-$PPEGMA_{70}$; the apparent core−shell morphology in Figure 3a was confirmed by negatively staining the outer shell with uranyl acetate (Figure 4). It is interesting to note that the shells are not uniformly dark, which may be caused by some domain formation of the PS blocks.

The spherical morphology is lost upon increasing the surfactant concentration as is clearly observed in Figure 3b for the latex containing 5.2 wt % of stabilizer. At higher concentrations of surfactant, i.e., at 5.5 and 7.2 wt %, small particles along with nonspherical particles are present (see Figure 3, c and d, respectively). Finally and as mentioned before, at high conversion coagulation took place in the case of the latex particles stabilized with 9.2 wt % of surfactant. The TEM images of the stable particles of the mixture are displayed in Figure 3e, and it is clear that these particles have a small diameter of around 90 nm.

To investigate these results, the analysis of the polymerization rate per particle, R_{pp}, can be very useful. The number of particles was calculated from the diameters obtained by TEM and the rate of polymerization was determined from the linear part of the kinetic plots. As shown in Table 1, the rate of polymerization per particle did not change significantly for surfactant concentrations of 3.2 or 5.2 wt %. However, a considerable decrease in the R_{pp} was observed in the emulsion polymerization using 5.5 and 7.2 wt %. More surprisingly, at a higher concentration of surfactant, 9.2 wt %, the R_{pp} is dramatically reduced. Furthermore, the molecular weight distributions of the final latex shift to lower molecular weights for increased particle numbers, as expected, with the appearance of additional low molecular weight populations in the situations where additional small particles are formed (see Table 1 and Figure 5).

The observations regarding particle morphology, particle size distribution, N_p, R_{pp}, and molecular weight distributions described above are consistent with a phase separation phenomenon between the PMMA particle and the PS hydrophobic segments of the block copolymer stabilizers. This phase separation is likely to occur at some stage during the polymerization as initially the block copolymer micelles will just be swollen with MMA (in which the PS block is soluble), but at some stage the PMMA content in the particles is so high that it will "push out" the PS block. From the described results it is clear that the extent

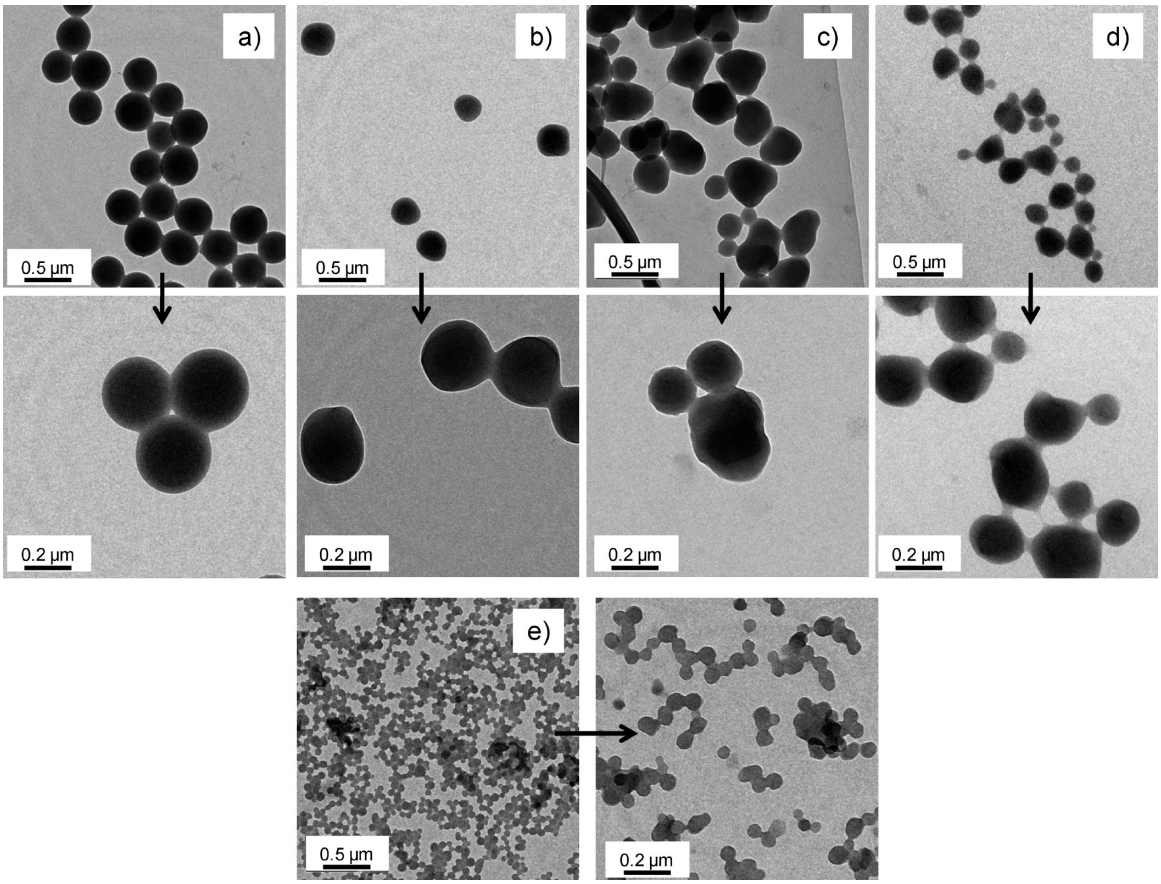

Figure 3. TEM images of PMMA latexes obtained via emulsion polymerization of MMA at 35 °C using (a) 3.2, (b) 5.2, (c) 5.5, (d) 7.2, and (e) 9.2 wt % of PS_{40}-*b*-$PPEGMA_{70}$ copolymer surfactant.

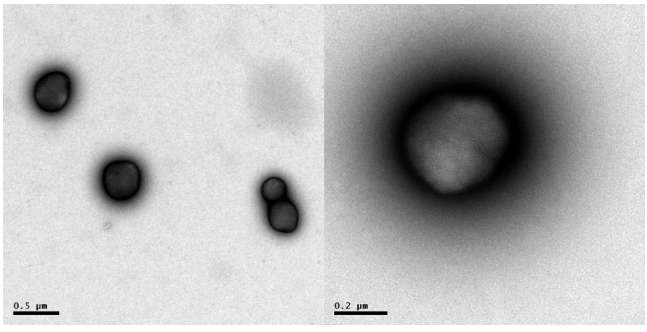

Figure 4. TEM images of PMMA latexes obtained via emulsion polymerization of MMA at 35 °C using 3.2 wt % of PS_{40}-*b*-$PPEGMA_{70}$ copolymer surfactant and negatively stained with uranyl acetate.

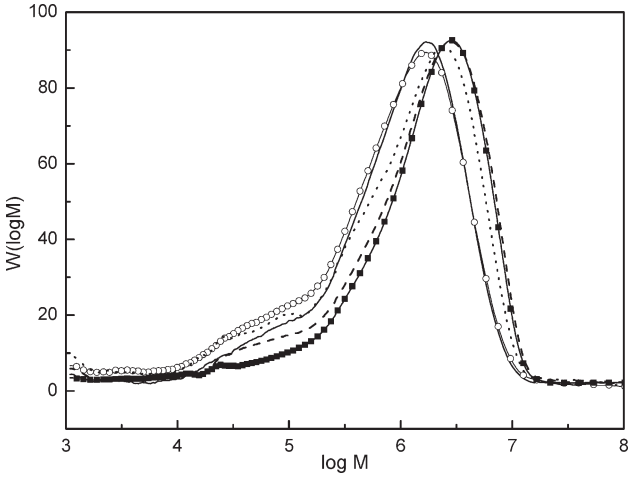

Figure 5. Molecular weight distributions of PMMA latexes obtained via emulsion polymerization of MMA at 35 °C using (■) 3.2, (---) 5.2, (···) 5.5, (○) 7.2, and (—) 9.2 wt % of PS_{40}-*b*-$PPEGMA_{70}$ copolymer surfactant.

to which this affects the polymerization process depends on the used block copolymer concentration. When a low concentration of polymeric surfactant was used, spherical and monodisperse core−shell particles were obtained. However, when the amount of PS_{40}-*b*-$PPEGMA_{70}$ was higher than 5.2 wt %, the particles started to become irregular and smaller particles were formed (broad particle size distributions were observed by DLS and TEM). The effects of the incompatibility of the polystyrene block and the PMMA particle matrix are more pronounced at higher concentrations of block copolymer surfactant where small particles were formed, enriched in PS_{40}-*b*-$PPEGMA_{70}$ copolymer. Especially from the results obtained at 9.2 wt % block copolymer, where TEM and DLS only show small particles enriched in block copolymer (measured on the latex after removal of the 10% coagulum), we conclude that the polymerization rate in the small particles is smaller. An obvious explanation of these results, however, is elusive. A lower concentration of MMA monomer present in the particles which now consist for a significant part of

dx.doi.org/10.1021/ma200626p |*Macromolecules* 2011, 44, 4282–4290

the PS of the block copolymer surfactant is likely, but not a sufficient reason to explain the order of magnitude drop in the R_{pp} (see Table 1) as compared to the systems with 5.5 and 7.2 wt % of block copolymer. Although a lower molecular weight would indeed be expected in the case of a lower monomer concentration, the observed decrease in Figure 5 is not sufficient. Additional effects may also include an increase in exit rate from the smaller particles or a somehow reduced entry rate.[30] It is clear that we still do not understand the full mechanism of the polymerization and that more detailed kinetic studies on particle formation and growth are required.

In contrast to these observations in the emulsion polymerization of MMA, we did not observe this behavior in our previous study on the emulsion polymerization of styrene stabilized with PS_{40}-*b*-$PPEGMA_{70}$, where spherical and monodisperse particles were observed at low concentration of polymer surfactant, 3.2 and 1.6 wt %.[5] Since in the previous article we did not use any higher amounts of surfactant, we extended the range of PS_{40}-*b*-$PPEGMA_{70}$ concentrations in the emulsion polymerization of styrene to 5.2 and 9.2 wt % in the current study. Figure 6 shows the kinetic plots of the emulsion polymerization of styrene with different amount of PS_{40}-*b*-$PPEGMA_{70}$. As expected, the rate of polymerization increases and the particle size decreases (Table 2) as the amount of surfactant increases; no coagulation was observed.

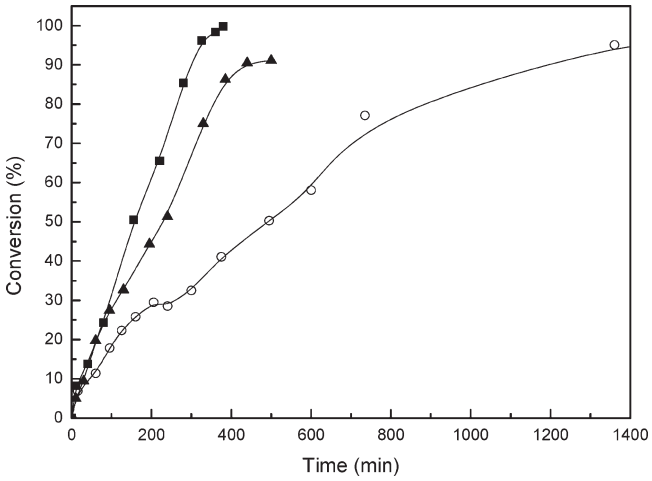

Figure 6. Evolution of monomer conversion with time for the emulsion polymerization of styrene using a redox initiator system ammonium persulfate/sodium thiosulfate (0.8 wt %) and (○) 3.2 (data taken from ref 5), (▲) 5.2, and (■) 9.2 wt % of PS_{40}-*b*-$PPEGMA_{70}$ block copolymer as stabilizer.

In addition, the particle sizes were also measured by TEM, obtaining the same correlation between the amount of PS_{40}-*b*-$PPEGMA_{70}$ stabilizer and the obtained diameter. Again, the sizes obtained by TEM are smaller than those obtained by DLS, and core−shell structures were observed as shown in Figure 7. Although it has been previously reported that the incompatibility effect reduces the particle size (the surfactant has less tendency to be entrapped and more surfactant molecules are able to act as stabilizer),[31] the obtained particle sizes are similar to those of the PMMA latex (Table 1). This similarity is conceivably explained by the fact that the emulsion polymerization was carried out at low temperature using a redox initiator system. Under these conditions the hydrophilicity of the nonionic block copolymer increases, and the incorporation of the block copolymer stabilizer inside the particle is significantly reduced.[32,5]

When considering the particle morphology, it is clear from Figure 7 that in this case the particles remain spherical in the whole range of surfactant concentrations. From these observations and the very similar rates of polymerization per particle and the obtained molecular weights (Table 2), it is safe to conclude that the polymeric surfactant behaves as expected in this emulsion polymerization. Hence, we can conclude that the miscibility between the hydrophobic segment of the block copolymer surfactant and the polymer forming the core of the particles is

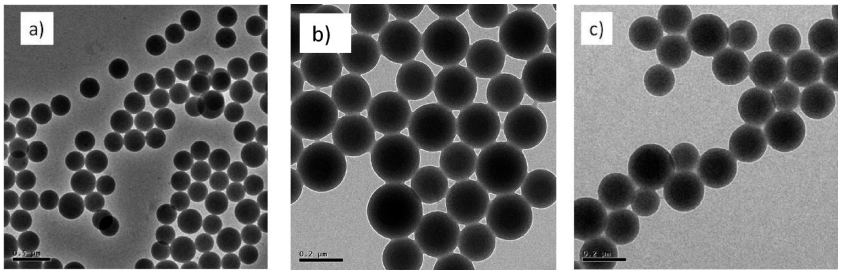

Figure 7. TEM images of polystyrene latexes obtained via emulsion polymerization of styrene at 35 °C using (a) 3.2, (b) 5.2, and (c) 9.2 wt % of PS_{40}-*b*-$PPEGMA_{70}$ block copolymer as stabilizer.

Table 2. Summary of Particle Size and Molecular Weight Data of the PS Latexes Stabilized with PS_{40}-*b*-$PPEGMA_{70}$ Surfactant

surfactant (wt %)	D_{DLS}[a] (nm)	$POLY_{DLS}$[b]	D_{TEM}[c] (nm)	PDI_{TEM}[d]	$M_w \times 10^{-5}$[e] (g mol^{-1})	$N_p \times 10^{-16}$[f] (L^{-1})	$R_{pp} \times 10^{17}$[g] (min^{-1})
3.2	367	0.08	286	1.09	7.9	1.3	0.3
5.2	343	0.03	179	1.02	7.5	5.3	0.2
9.2	289	0.02	151	1.02	7.9	8.8	0.7

[a] *Z*-average particle diameter obtained from DLS using Malvern Dispersion Technology Software for data acquisition and analysis, applying the general purpose algorithm for calculating size distributions. [b] Associated normalized coefficient of variation. [c] Number-average particle diameter determined from TEM using the software ImageJ. [d] Polydispersity index of the particle size distribution determined via TEM: $PDI_{TEM} = D_w/D_n$, where D_w is the weight-average diameter, $D_w = \Sigma n_i D_i^4/\Sigma n_i D_i^3$, and D_n is the number-average diameter, $D_n = \Sigma n_i D_i / n_i$ (n_i is the number of particles with diameter D_i). [e] Weight-average molecular weight of the product polymer determined by SEC relative to PS standards. [f] N_p = number of particles per liter latex. [g] R_{pp} is the rate of polymerization per particle, here defined as $R_{pp} = R_p/N_p$, where R_p is the rate of polymerization.

dx.doi.org/10.1021/ma200626p |*Macromolecules* 2011, 44, 4282–4290

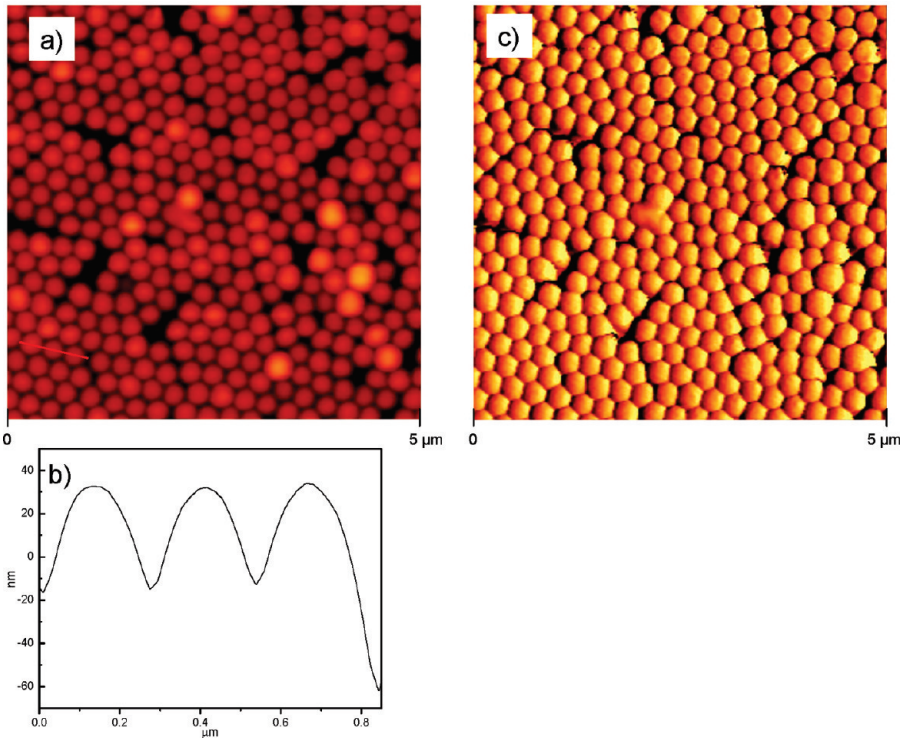

Figure 8. AFM images of polystyrene latex obtained via emulsion polymerization of styrene at 35 °C using 3.2 wt % of PS_{40}-*b*-$PPEGMA_{70}$ block copolymer as stabilizer: (a) height image and (b) its corresponding cross section; (c) phase image.

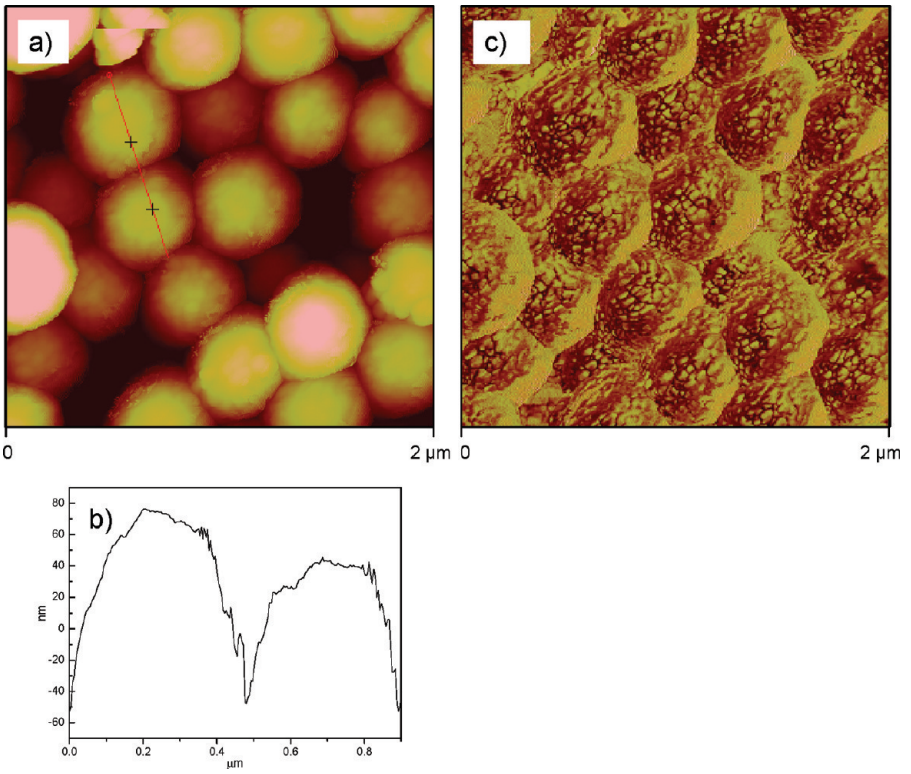

Figure 9. AFM images of poly(methyl methacrylate) latex obtained via emulsion polymerization of methyl methacrylate at 35 °C using 3.2 wt % of PS_{40}-*b*-$PPEGMA_{70}$ block copolymer as stabilizer: (a) height image and (b) its corresponding cross section; (c) phase image.

quite important in the morphology of the final particles and in the mechanism of the emulsion polymerization.

Both systems of hairy particles (i.e., those containing a PS or PMMA core) were further imaged by atomic force microscopy in

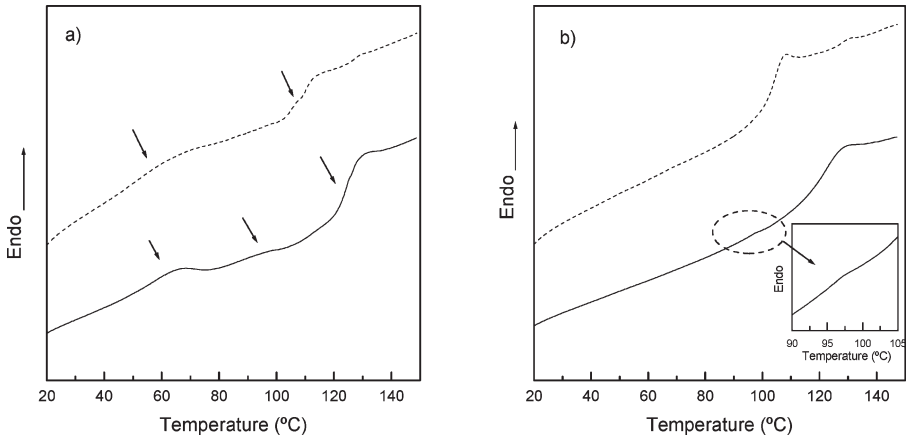

Figure 10. DSC thermograms of (---) PS latex and (—) PMMA latex with 5.2 wt % of PS_{40}-*b*-$PPEGMA_{70}$ during the (a) first heating scan and (b) second heating scan.

Table 3. Glass Transition Temperatures and Melting Temperature of PS and PMMA Latex Containing PS_{40}-*b*-$PPEGMA_{70}$ Block Copolymer as Stabilizer Obtained from DSC Measurements[a]

		first heating			second heating		
latex	PS_{40}-*b*-$PPEGMA_{70}$ (wt %)	T_m (°C) $PPEGMA_{70}$	T_{g1} (°C) PS_{40}	T_{g2} (°C) matrix	T_m (°C) $PPEGMA_{70}$	T_{g1} (°C) PS_{40}	T_{g2} (°C) matrix
PS	3.2	59.0	–	108.5	–	–	103.5
	5.2	56.0	–	110.5	–	–	103.0
	9.2	55.5	–	107.5	–	–	103.0
PMMA	3.2	58.5	87.0	123.0	–	91.5	116.5
	5.2	57.0	87.5	124.5	–	92.0	119.0
	5.5	53.5	82.5	124.0	–	92.0	117.0
	7.2	55.0	84.0	129.0	–	91.0	123.5
	9.2	56.5	84.5	124.0	–	90.0	113.5

[a] Temperature standard error ±0.5 °C.

order to study in detail the roughness of the particle surface. AFM has been applied previously to study the surface morphology of core−shell latex particles.[33,34] The topographic images (Figure 8) of the PS particles stabilized with 3.2 wt % of PS_{40}-*b*-$PPEGMA_{70}$ showed a regular array of ordered particles, which confirms the narrow particle size distribution.

The height image, the corresponding cross section, and the phase image indicate that the surface of the particles is quite smooth. In contrast, the AFM images (Figure 9) of the PMMA particles containing 3.2 wt % of PS_{40}-*b*-$PPEGMA_{70}$ reveal certain roughness of the particle surface, appearing somewhat "wrinkled". This roughness found on the PMMA particles can again be attributed to the immiscibility and phase separation between the PMMA core and the hydrophobic PS segments of the block copolymer surfactant.

Once we demonstrated that the incompability and the phase separation between the growing polymer particle and the hydrophobic segment of the block copolymer affect the emulsion polymerization mechanism and the particle morphology, we investigated its effect on the film formation of both latex systems by AFM and DSC. First, the dried particles of PMMA and PS containing the block copolymer stabilizers were characterized by DSC. Figure 10a shows the DSC thermograms during the first heating scan to 150 °C, and the results are summarized in Table 3. Latex particles of PS show two distinct transitions, a broad melting point at $T_m \sim 55$ °C which corresponds to the

Figure 11. Images of films formed after annealing at 150 °C during 24 h, from PS latex stabilized with 3.2 wt % of PS_{40}-*b*-$PPEGMA_{70}$ (left film) and PMMA latex stabilized with 3.2 wt % of PS_{40}-*b*-$PPEGMA_{70}$ (right film).

$PPEGMA$[35] segments of the block copolymer and the glass transition temperature of the PS core, $T_{g2} \sim 110$ °C, whereas the latex particles of PMMA present three transitions, $T_m \sim 55$ °C, $T_{g1} \sim 85$ °C, and $T_{g2} \sim 125$ °C, corresponding to the T_g of the PMMA core ($T_{g2} \sim 125$ °C), the T_g of the PS block, $T_{g1} \sim 85$ °C,[36] and the broad T_m of the PPEGMA in the block copolymer surfactant PS_{40}-*b*-$PPEGMA_{70}$. These results support

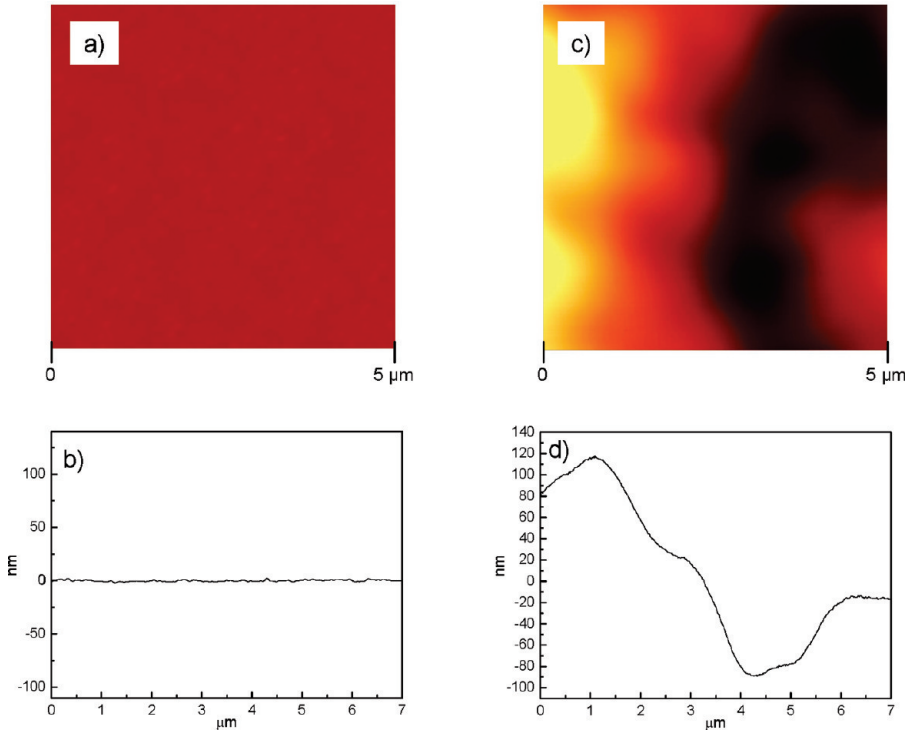

Figure 12. (a) AFM height image and (b) its corresponding cross section of a polystyrene latex film containing 3.2 wt % of PS_{40}-*b*-$PPEGMA_{70}$ block copolymer. (c) AFM height image and (d) its corresponding cross section of a poly(methyl methacrylate) latex film containing 3.2 wt % of PS_{40}-*b*-$PPEGMA_{70}$ block copolymer.

the earlier assessment of the incompatibility and the phase separation between the polystyrene hydrophobic block of polymeric surfactant and the PMMA core.

In contrast to the results obtained for the PMMA particles, only the T_m of the PPEGMA block and the T_{g2} of the PS core were detected in the first heating scan of the PS particles. In this case the glass transition temperature of PS blocks in the copolymers was not distinguishable from that of the core because phase separation does not occur. The second heating run of the PS and PMMA latex samples were carried out and the results are displayed in Figure 10b and summarized in Table 3. After the first heating to 150 °C, where the coalescence of the particles is expected, the samples were cooled down at the same rate (10 °C/min), and a second heating run was performed. Only one T_g was found in the DSC trace of the PS samples. This T_g corresponds to the polystyrene core, acquiring a value slightly shifted to lower temperature compare to the T_g obtained during the first heating. The T_m of the PPEGMA was not observed because the sample was cooled down to 10 °C, and the crystallization temperature in this case is lower.[37] The block copolymer surfactant induces a decrease in the T_g of the polystyrene latex matrix due to the plasticizing effect. Contrasting this with the two T_gs were observed in the DSC curves of the PMMA samples, the glass transition of the polystyrene segment of the copolymer is visible in addition to the T_g of the PMMA, implying the occurrence of phase separation. Again, in the second heating scans the T_m of PPEGMA is not observed, and a decrease in the T_g of the PMMA matrix is observed.

Latex films were prepared from both PS and PMMA particles containing different amounts of copolymer stabilizer at room temperature and subsequently annealed at 150 °C (i.e., above the highest observed glass transition temperature) allowing the coalescence of the particles. Figure 11 shows a comparison of the transparency of the PS and PMMA films, both containing 3.2 wt % of PS_{40}-*b*-$PPEGMA_{70}$ after the annealing. It can be clearly seen that PS latex film can form a transparent film whereas the PMMA films are opaque white with small cracks.

Furthermore, the surface morphology of these films was studied by AFM. The images (Figure 12a,b) show that the surface of the film formed from the PS particles stabilized with PS_{40}-*b*-$PPEGMA_{70}$ is relatively smooth and flat, revealing that the whole surface consists of a single phase. In contrast the surface of the films obtained from the PMMA latex particles appears significantly rougher (Figure 12c,d). The quality of composite latex film depends on many factors such as molecular weight, surfactants, polydispersity, particle sizes, morphologies of the particles, miscibility, or phase separation between the different components and film formation conditions.[38−43,26,27] In this case the turbidity and roughness of the films formed from PMMA latex particles could be attributed to the incompatibility of PMMA core and the polystyrene hydrophobic segment of the block copolymer stabilizer. Since the PS and PMMA are indeed immiscible polymers, a phase separation can occur during the coalescence of the PMMA core, which leads to opaque films. This feature has been previously observed on both composite latexes and particles stabilized with polymer surfactant.[44,45,29,28,41]

CONCLUSIONS

The synthesis of hairy latex particles of PMMA and PS using a brush type amphiphilic block copolymer of polystyrene-*b*-poly-[poly(ethylene glycol) methyl ether methacrylate] (PS_{40}-*b*-$PPEGMA_{70}$) as stabilizer has been reported. The incompatibility or miscibility between the core of the particles (PS or PMMA) and the hydrophobic block of the surfactant (PS) affects the

kinetics and the mechanism of the emulsion polymerization. Furthermore, in the case of the PMMA latex particles, irregular morphologies are obtained because of the phase separation between the growing polymer particle or the core and the PS segment of the block copolymer surfactant; the obtained particle morphology depends of the concentration of the block copolymer stabilizers. The incompatibility between the polymeric surfactant and the latex particle also influences the formation of the films, resulting in opaque films with a rough surface. In contrast, spherical and monodisperse core−shell particles are produced in the emulsion polymerization of styrene stabilized with the block copolymer surfactant where the hydrophobic block of the surfactant is compatible with the core of the particles and smooth transparent films are formed from these latexes.

AUTHOR INFORMATION

Corresponding Author

*E-mail: j.p.a.heuts@tue.nl.

ACKNOWLEDGMENT

This work was financially supported by the Foundation Emulsion Polymerization (SEP) and by the Ministerio de Ciencia e Innovación (Project MAT2010-17016). A. Muñoz-Bonilla gratefully acknowledges MICINN-CSIC for her post-doctoral grant, and S. I. Ali gratefully acknowledges the financial support by the Higher Education Commission, Government of Pakistan, under the HEC-NUFFIC program.

REFERENCES

(1) Riess, G.; Labbe, C. *Macromol. Rapid Commun.* **2004**, *25*, 401–435.
(2) Burguiere, C.; Chassenieux, C.; Charleux, B. *Polymer* **2003**, *44*, 509–518.
(3) Save, M.; Manguian, M.; Chassenieux, C.; Charleux, B. *Macromolecules* **2005**, *38*, 280–289.
(4) Tan, B.; Nabuurs, T.; Feijen, J.; Grijpma, D. W. *J. Polym. Sci., Part A: Polym. Chem.* **2009**, *47*, 4234–4244.
(5) Muñoz-Bonilla, A.; van Herk, A. M.; Heuts, J. P. A. *Macromolecules* **2010**, *43*, 2721–2731.
(6) Gonzalez-Ortiz, L. J.; Asua, J. M. *Macromolecules* **1995**, *28*, 3135–3145.
(7) Gonzalez-Ortiz, L. J.; Asua, J. M. *Macromolecules* **1996**, *29*, 383–389.
(8) Herrera, V.; Palmillas, Z.; Pirri, R.; Reyes, Y.; Leiza, J. R.; Asua, J. M. *Macromolecules* **2010**, *43*, 1356–1363.
(9) Herrera, V.; Pirri, R.; Asua, J. M.; Leiza, J. R. *J. Polym. Sci., Part A: Polym. Chem.* **2007**, *45*, 2484–2493.
(10) Stubbs, J. M.; Sundberg, D. C. *J. Coat. Technol. Res.* **2008**, *5*, 169–180.
(11) Lee, D. I.; Ishikawa, T. *J. Polym. Sci., Polym. Chem. Ed.* **1983**, *21*, 147–154.
(12) Sheu, H. R.; El-Aasser, M. S.; Wanderhoff, J. W. *J. Polym. Sci., Part A: Polym. Chem.* **1990**, *28*, 653–667.
(13) Okubo, M.; Nakagawa, T. *Colloid Polym. Sci.* **1994**, *272*, 45–51.
(14) Wei, R.; Luo, Y.; Li, Z. *Polymer* **2010**, *51*, 3879–3886.
(15) Eckersley, S. T.; Rudin, A. In *Film Formation in Waterborne Coatings*; Provder, T., Winnik, M. A., Urban, M. W., Eds.; ACS Symposium Series 648; American Chemical Society: Washington, DC, 1996; p 2.
(16) Niu, B. J.; Martin, L. R.; Tebelius, L. K.; Urban, M. W. In *Film Formation in Waterborne Coatings*; Provder, T., Winnik, M. A., Urban, M. W., Eds.; ACS Symposium Series 648; American Chemical Society: Washington, DC, 1996; p 301.
(17) Keddie, J. L.; Meredith, P.; Jones, R. A. L.; Donald, A. M. In *Film Formation in Waterborne Coatings*; Provder, T., Winnik, M. A., Urban, M. W., Eds.; ACS Symposium Series 648; American Chemical Society: Washington, DC, 1996; p 332.
(18) Ming-Da, Eu; Ullman, R. In *Film Formation in Waterborne Coatings*; Provder, T., Winnik, M. A., Urban, M. W., Eds.; ACS Symposium Series 648; American Chemical Society: Washington, DC, 1996; p 79.
(19) Winnik, M. A. In *Film Formation in Waterborne Coatings*; Provder, T., Winnik, M. A., Urban, M. W., Eds.; ACS Symposium Series 648; American Chemical Society: Washington, DC, 1996; p 51.
(20) Feng, J. R.; Winnik, M. A. *Macromolecules* **1997**, *30*, 4324–4331.
(21) Ma, Y.; Davis, H. T.; Scriven, L. E. *Prog. Org. Coat.* **2005**, *52*, 46–62.
(22) Keddie, J. L.; Meredith, P.; Jones, R. A.; Donald, A. M. *Langmuir* **1996**, *12*, 3793–3801.
(23) Meincken, M.; Sanderson, R. D. *Polymer* **2002**, *43*, 4947–4955.
(24) Dreher, W. R.; Jarret, W. T.; Urban, M. W. *Macromolecules* **2005**, *38*, 2205–2212.
(25) Otts, D. B.; Dutta, S.; Zhang, P.; Smith, O. W.; Thames, S. F.; Urban, M. W. *Polymer* **2004**, *45*, 6235–6243.
(26) Park, Y. J.; Khew, M. C.; Ho, C. C.; Kim, J. H. *Colloid Polym. Sci.* **1998**, *276*, 709–714.
(27) Yuan, X.; Huo, D.; Qian, Q. *J. Colloid Interface Sci.* **2010**, *346*, 72–78.
(28) Schantz, S.; Carlsson, H. T.; Andersson, T.; Erkselius, S.; Larsson, A.; Karlsson, O. J. *Langmuir* **2007**, *23*, 3590–3602.
(29) Ugur, S.; Elaissari, A.; Holl, Y. *Polym. Compos.* **2006**, *27*, 431–442.
(30) Gilbert, R. G. *Emulsion Polymerization. A Mechanistic Approach*; Academic Press: London, UK, 1995.
(31) Riess, G. *Colloids Surf., A* **1999**, *153*, 99–110.
(32) Okubo, M.; Kobayashi, H.; Matoba, T.; Oshima, Y. *Langmuir* **2006**, *22*, 8727–8731.
(33) Sommer, F.; Duc, T.; Piiri, R.; Meunier, G.; Quet, C. *Langmuir* **1995**, *11*, 440–448.
(34) Stubbs, J. M.; Sundberg, D. C. *Polymer* **2005**, *46*, 1125–1138.
(35) Neugebauer, D.; Zhang, Y.; Pakula, T.; Sheiko, S. S.; Matyjaszewski, K. *Macromolecules* **2003**, *36*, 6746.
(36) O'Driscoll, K.; Sanayei, R. A. *Macromolecules* **1991**, *24*, 4479–4480.
(37) Neugebauer, D.; Zhang, Y.; Pakula, T.; Matyjaszewski, K. *Macromolecules* **2005**, *38*, 8687–8693.
(38) Cannon, L. A.; Pethrick, R. A. *Macromolecules* **1999**, *32*, 7617–7629.
(39) Ugur, S.; Pekcan, O. *Colloid Polym. Sci.* **2005**, *284*, 309–316.
(40) Huijs, F.; Lang, J. *Colloid Polym. Sci.* **2000**, *278*, 746–756.
(41) Colombini, D.; Ljungberg, N.; Hassander, H.; Karlsson, O. J. *Polymer* **2005**, *46*, 1295.
(42) Misra, A.; Jarrett, W. L.; Urban, M. W. *Macromolecules* **2009**, *42*, 7299–7308.
(43) Cannon, L. A.; Pethrick, R. A. *Polymer* **2002**, *43*, 6429–6438.
(44) Pekan, O.; Arda, E.; Kesenci, K.; Piskin, E. *J. Appl. Polym. Sci.* **1998**, *68*, 1257–1267.
(45) Otts, D. B.; Dutta, S.; Zhang, P.; Smith, O. W.; Thames, S. F.; Urban, M. W. *Polymer* **2004**, *45*, 6235–6243.